JOURNAL OF MATERIALS SCIENCE 26 (1991) 6753–6758

Transmission electron microscopic study of three-dimensional polyacrylonitrile fibre-mesophase pitch matrix carbon–carbon composite

C. P. JU, J. DON, P. TLOMAK
Materials Technology Center, Southern Illinois University at Carbondale, Carbondale, IL 62901-4303, USA

Conventional and high resolution transmission electron microscopy performed in this study provides some detailed microstructural information of a polyacrylonitrile (PAN) fibre-mesophase pitch matrix carbon–carbon composite which has not been published in open literature. The PAN fibre in this composite possesses a turbostratic structure throughout the fibre. The structure of the mesophase pitch matrix is graphitic and anisotropic. Near-fibre matrix crystallites are aligned roughly parallel to the fibre surface, exhibiting a flow-type morphology. The fibre–matrix interface in this composite is microfissured. Numerous microcracks exist both within the matrix and along partially bonded interfaces. The irregularly shaped interfacial microcracks readily expose the fibre surface topography. Microcracks within the matrix are formed between, and parallel to, the basal planes of the graphitic platelets. Such submicron-sized matrix cracks appear smaller and denser near the fibre–matrix interface.

1. Introduction

The unique properties of carbon–carbon (C–C) composites, such as high heat of ablation, high temperature strength, thermal shock resistance, chemical inertness and compatibility with human tissues, have drawn the attention of many materials scientists and engineers. These exceptional properties coupled with light weight suggest many aeronautical, aerospace, industrial and biomedical applications, including reentry vehicle heat shields, solid rocket motor nozzles, aircraft brake discs, high temperature crucibles and surgical implants. The high temperature stability and "low-Z" feature have also made C–C a strong candidate for the first wall material of fusion reactors, although some problems, such as poor radiation response, high tritium inventories and gasification, are yet to be solved.

In spite of the many conventional transmission electron microscopy (CTEM) and high resolution electron microscopy (HREM) studies on carbon fibres [1–6], mesophase [7–10], and other carbonaceous materials [4, 11–15], little TEM work [16] on carbon–carbon composites has been published in open literature. The present work presents TEM results of a commercial, three-dimensional PAN fibre-mesophase pitch matrix carbon–carbon composite which has been used as a rocket nozzle. Bright field (BF), dark field (DF), selected area diffraction (SAD) and HREM techniques were performed to characterize the microstructure of the composite in some detail. This microstructural information would hopefully help understand properties of such a composite.

2. Experimental procedure

T-300 PAN fibres were used to reinforce a mesophase coal tar pitch matrix in a commercial, three-dimensional carbon–carbon composite. Following pressurized molten pitch impregnation, the composite was carbonized and graphitized. To meet the desired density and properties, the impregnation/carbonization/graphitization cycle was repeated several times. The detailed process parameters were not released due to proprietary consideration.

Preparation of the carbon–carbon thin foils for TEM involved mechanical dimpling followed by argon atom milling. Specimens about 0.5 mm thick were sliced from the bulk composite using a diamond saw. 3 mm diameter discs were cut from each slice using a press drill. Such discs were mechanically dimpled (VCR Group D500 mechanical dimpler) to a thickness of roughly 10 μm (a 0.5 μm diamond paste was used for the final stage of dimpling). The dimpled discs were then atom milled (ION TECH FAB 306 atom miller) at liquid nitrogen temperature. A beam current of 1 mA and an initial incident angle of 25–30° were used. After roughly 48 hours of milling, the bombarding angle was lowered to 10–12° until perforation.

3. Results and discussion

3.1. The fibre

The basal plane orientation of the PAN fibres in the present composite was essentially turbostratic in nature. In transverse sections, the turbostratic structure, as shown in Fig. 1a and c, exists across the

0022–2461/91 $03.00 + .12

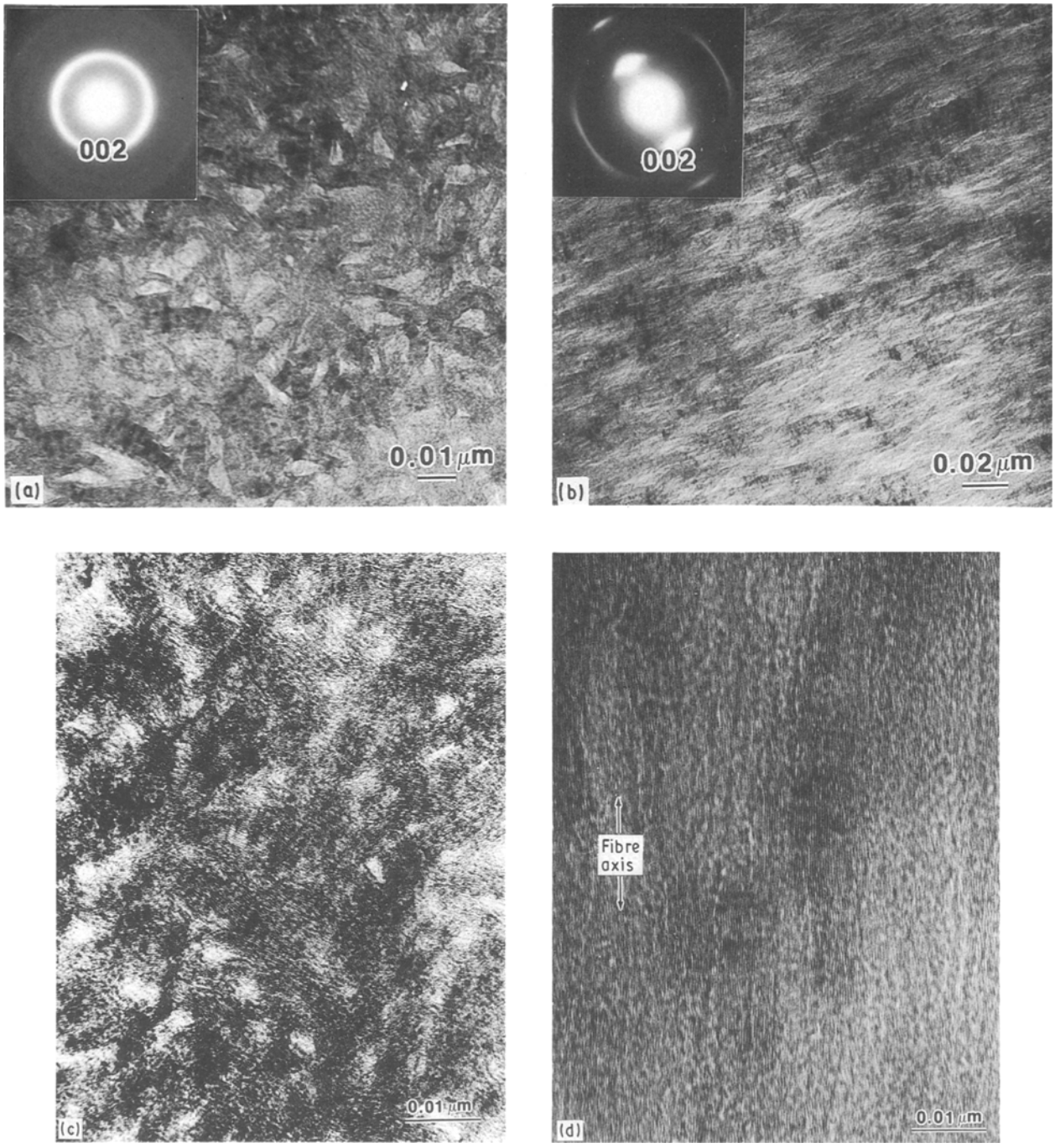

Figure 1 Microstructure and basal plane orientation of PAN fibre. (a) BF, transverse section; (b) BF, longitudinal section; (c) high resolution basal plane fringes, transverse section and (d) high resolution basal plane fringes, longitudinal section.

whole fibre thickness. In longitudinal sections, the degree of perfection for basal plane alignment to the fibre axis decreases from fibre surface to fibre core in a gradual manner. A typical microstructure as well as basal plane alignment in a longitudinal section are shown in Fig. 1b and d, respectively. Detailed microstructure and basal plane orientation of the PAN fibres used in the present composite has been reported elsewhere [17].

3.2. The matrix

Like fibre basal plane orientation, the matrix basal plane orientation also plays an important role in deciding the properties of C–C composites [18, 19]. A typical transverse morphology within a fibre bundle of this composite is shown in Fig. 2a. The morphological differences between the matrix and the fibres are significant in this low magnification, BF micrograph. The intrabundle matrix crystallites are oriented roughly parallel to the fibre surface, exhibit a flow type morphology, as indicated in Zimmer and White's model [20] which is based on polarized light microscopic examination. The crystallites near fibre surfaces or between closely spaced fibres have better alignment (parallel to the fibre surface) than those far from fibres. Numerous microfissures, generated during fabrication, are clearly revealed within the matrix as well as along the fibre–matrix interface.

Cranmer *et al.* [21] have suggested that the alignment of the mesophase material adjacent to a mesophase–substrate interface is primarily controlled

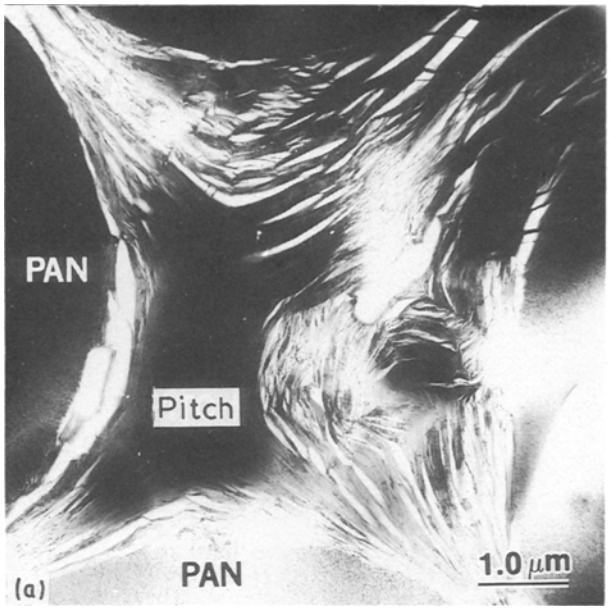

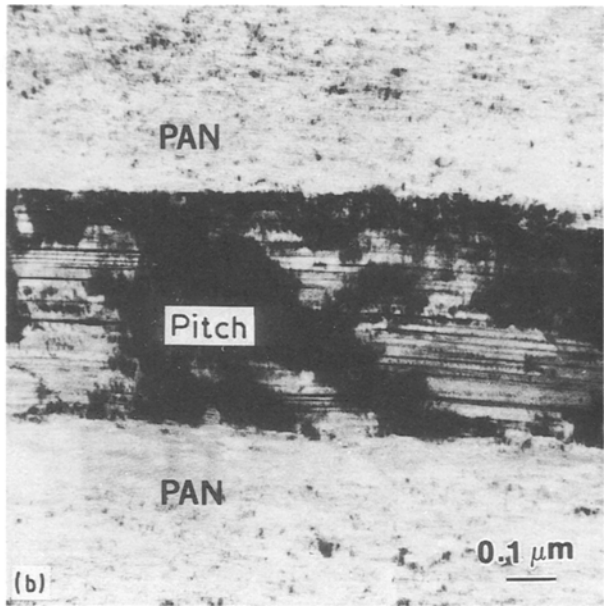

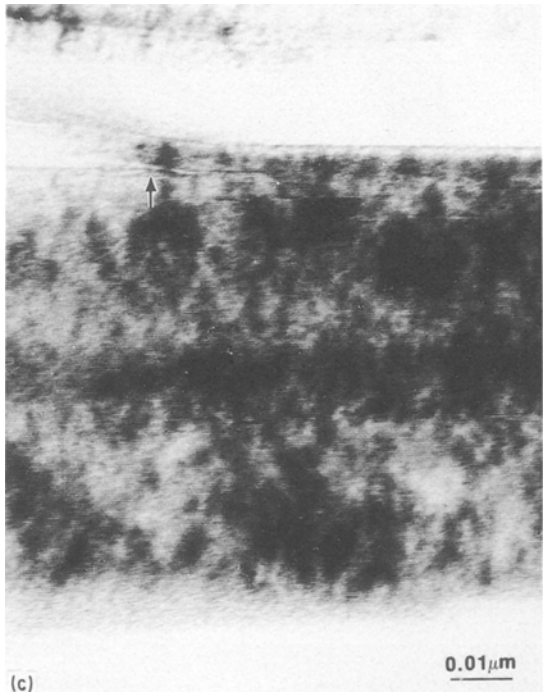

Figure 2 Microstructure and basal plane orientation of intrabundle mesophase pitch matrix. (a) BF, transverse section; (b) BF, longitudinal section; (c) high resolution basal plane fringes, longitudinal section.

by the flow motion of mesophase spherules. Although this circumferential, sheath-like morphology is most commonly observed in pitch-based C–C composites, a transversely aligned morphology of intrabundle matrix has also been observed [22]. The morphological differences between sheath-like and transversely aligned matrices have been attributed to the difference in impregnation pressure. High pressures were reported to produce a transversely aligned matrix, whereas low pressures produced a sheath-like matrix [22]. A study performed by Murdie *et al.* [23], however, indicated that a transversely aligned intrabundle matrix could also be produced under an atmospheric carbonization condition. It seems that pressure is not the only factor determining the intrabundle matrix morphology (circumferential or transverse).

The BF micrograph, Fig. 2b, shows a longitudinal morphology of an intrabundle matrix region. The crystallites in the pitch matrix are apparently much larger and more graphitic than in the turbostratic PAN fibre. It is interesting to note that this matrix region, though thin (≈ 0.5 μm), is not a single crystallite, but comprises a larger number of much thinner crystallites, each of which has a thickness of roughly 0.01 to 0.02 μm. Fig. 2c shows high resolution basal plane fringes in a longitudinal section of such a region. This lattice image was obtained using a common tilted-beam DF technique. Compared to those in PAN fibres (Fig. 1d), the basal planes in matrix crystallites are much better aligned. An example of crystallite splitting as well as basal plane bending, which serves as a major mechanism in crystallite boundary formation, is also shown in this lattice image. A similar basal plane alignment was found in a commercial mesophase pitch fibre [24]. The difference in basal plane alignment between those mesophase pitch fibres and the present PAN fibres are attributed to their different moduli and other properties. Usually, the more "straightened out" basal planes in mesophase pitch fibres reflect a greater modulus.

Typical edgewise (in terms of the geometry of graphitic platelets) morphology of the matrix between fibre bundles is shown in Fig. 3. Within a single mesophase domain, such as that shown in this region, all the graphitic crystallites are roughly parallel, similar to the bulk mesophase morphology described in numerous published articles. The selected-area (≈ 1 μm in diameter) diffraction pattern, Fig. 3c, indicates the parallel of the basal planes to the fibre bundle direction.

Typical broad-face morphology of interbundle matrix platelets is shown in Fig. 4. The BF micrograph, Fig. 4a, exhibits a "replica-like" morphology. The granular feature is thought to be a result of sputter etching. The fine striations (marked by arrows) within

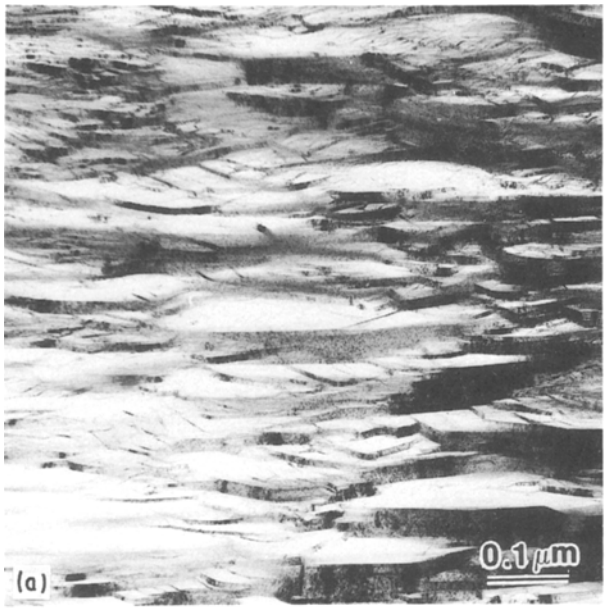

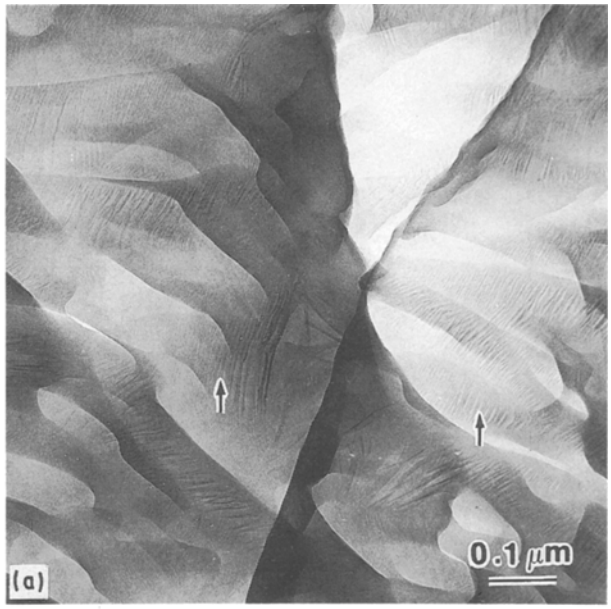

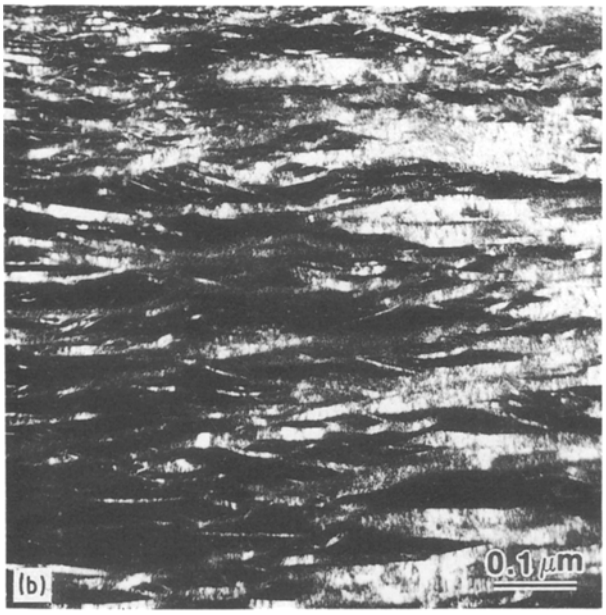

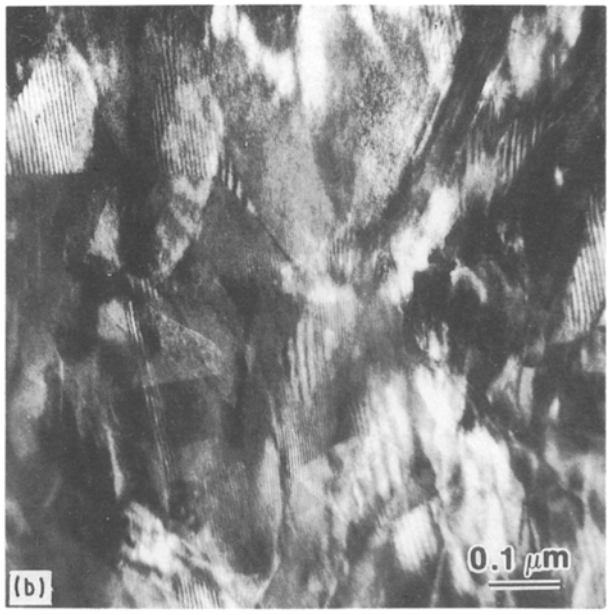

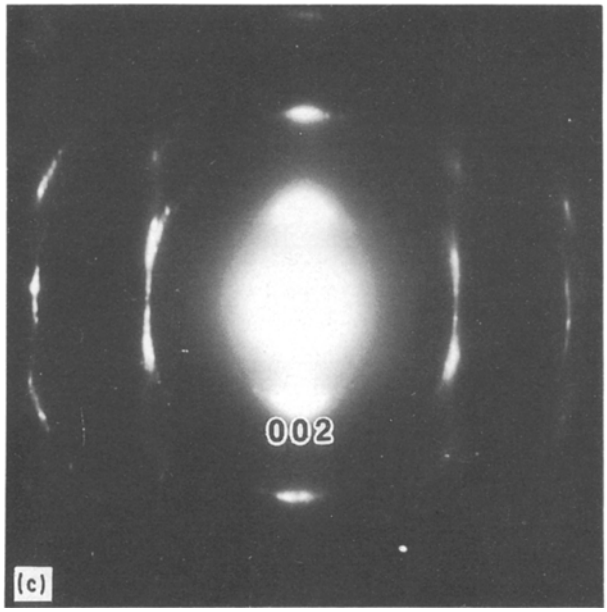

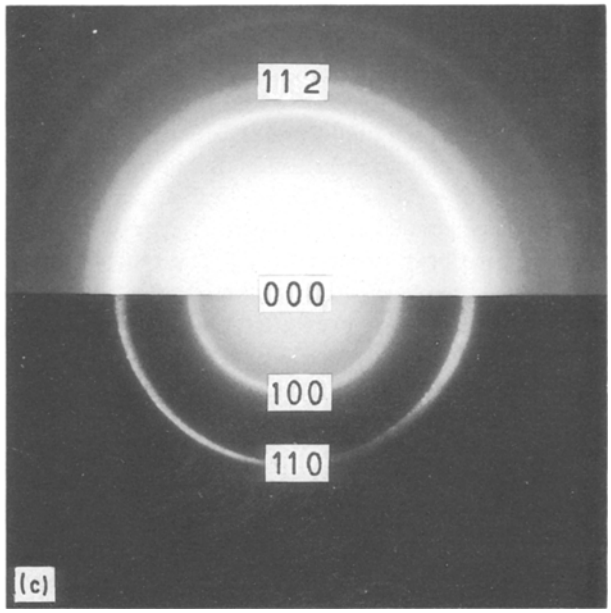

Figure 3 Edgewise morphology of interbundle matrix. (a) BF; (b) DF; (c) SAD pattern.

Figure 4 Broad-face morphology of interbundle matrix. (a) BF; (b) DF; (c) SAD pattern. Note the absence of basal plane rings.

each "grain" are possibly atom milling-induced ledges of basal planes. The DF micrograph of the same area, Fig. 4b, shows more clearly the crystallite shape and size (0.1–0.5 μm). The actual crystallite sizes, however, are probably much larger than those sketched by the rotation type Moire fringes due to an overlapping effect. Such Moire fringe morphology has been observed earlier by Rouzaud *et al.* [14] and Goma and Oberlin [13] in graphitized vapour-deposited carbon films as well as massive pyrocarbons. This type of morphology, to the author's knowledge, has not yet been reported in carbon–carbon composites. The absence of basal planes, such as (0 0 2) and (0 0 4), in the SAD pattern (a double exposure was used to reveal better the weak (1 1 2) ring), Fig. 4c, confirms that the basal planes of the crystallites are perpendicular to the incident electron beam.

3.3. The fibre–matrix interface

Fibre–matrix interactions are one of the most important issues for C–C, and, actually, for all kinds of fibre-reinforced composites. Fibre–matrix interactions in C–C composites can occur during infiltration/carbonization/graphitization process cycles as well as during applications (e.g., subjected to thermal and/or mechanical loading). The bonding (chemical, physical and mechanical) between matrix and fibres is a key factor in determining the properties of a C–C composite. It is known that too strong a bond may cause brittle failure of a C–C composite, whereas too weak a bond may lead to extensive fibre pullout and an insufficient stress transfer. Generally, a moderately weak bond between fibres and matrix is preferred for C–C composites [25–27].

The fibre–matrix interface in the present composite is generally discontinuous. Some matrix graphitic platelets are well bonded (the chemical nature of the bonding remains uncertain) to the fibre, whereas other platelets are poorly bonded or even entirely separated from the fibre. This interfacial morphology is somewhat similar to the "fissured type" interface as classified by Ragan and Marsh [28] in their study of bulk binder coke-filler coke composites.

A typical example of this partially bonded interface is shown in Fig. 5. In the DF micrograph, Fig. 5(a), two mesophase domains (marked "A" and "B", respectively) with different crystallite orientations are observed in the intrabundle matrix region. Within each domain, the graphitic platelets are aligned roughly parallel to the nearest fibre surface, as discussed earlier in Section 3.2. The higher magnification BF micrograph, Fig. 5b (the region marked "C" in Fig. 5a), clearly reveals the shape, size and distribution of the numerous microcracks along and near the fibre–matrix interface. The microcracks along the interface have an irregular shape which readily reveal the fibre surface topography. The microcracks within the matrix are formed between graphitic crystallite platelets (the basal planes in the platelets are parallel to the platelet broad faces, as identified by SAD) and have a sharp, lenticular shape. These submicron-sized inter–basal plane cracks appear smaller and denser

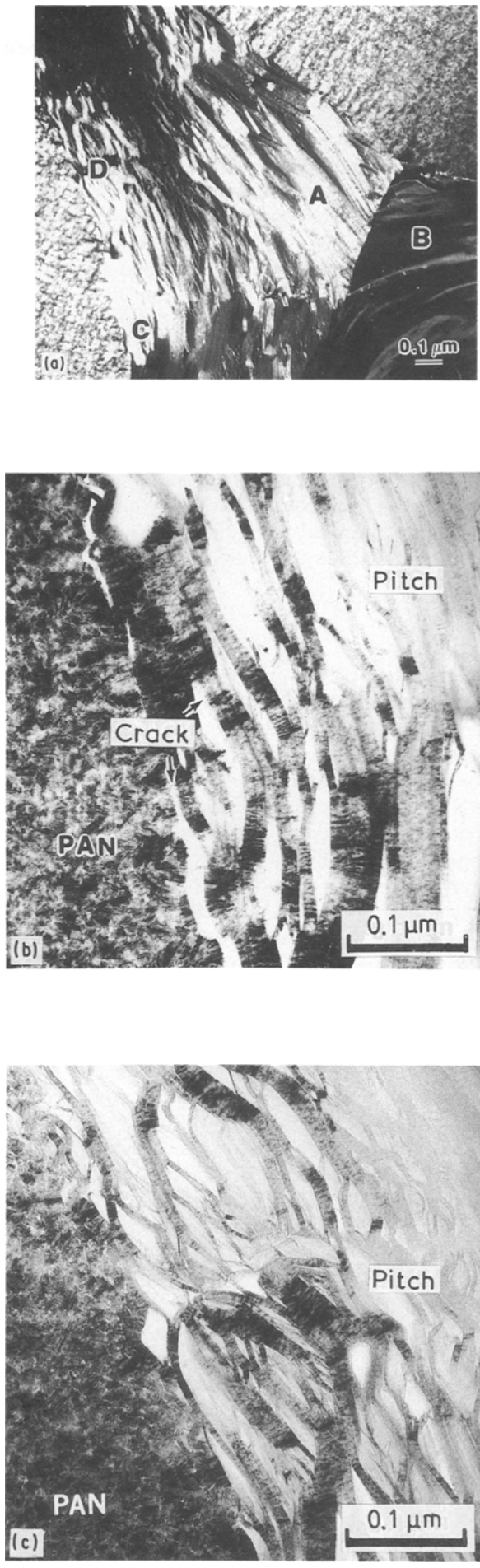

Figure 5 Fibre–matrix interface and near-interface matrix morphology. (a) DF, transverse section; (b) BF, higher magnification of region 'C'; and (c) BF, higher magnification of region 'D'.

when they are near the fibre surface. Such circumferential microcracks surrounding the fibres have been suggested by Sohn *et al.* [29] to be capable of increasing toughness of a chemical vapour infiltration (CVI)-based C–C composite. Although mechanical property data of the present PAN-pitch composite is not available, the numerous circumferential microcracks are thought able to play a similar role, i.e., to increase the composite toughness by deviating the paths (thus absorbing more energy) of advancing cracks.

The BF micrograph, Fig. 5c (the region marked "D" in Fig. 5a), only $\approx 0.5\ \mu m$ away from the region of Fig. 5b, exhibits a markedly different near-interface matrix morphology. The matrix crystallites appeared thinner, more random and more bent than in Fig. 5b. Since the fibre structure and surface roughness in the two regions are essentially the same, the different near-interface matrix morphologies are thought to be the result of differences in their flow nature during mesophase transition, which, in turn, is sensitive to the local three-dimensional geometry of the fibre preform in the composite.

4. Conclusions

Conventional and high resolution transmission electron microscopy in this study provides some detailed microstructural information which has not been published in open literature. The PAN fibre of the present PAN-pitch composite possesses a transversely turbostratic structure across the whole fibre thickness. In longitudinal sections, the degree of perfection for basal plane alignment to the fibre axis decreases from fibre surface to fibre core in a gradual fashion.

The crystallites of the mesophase pitch matrix are much larger and more graphitic than in the PAN fibre. The matrix platelets are aligned roughly parallel to the nearest fibre surface and have a smaller size than those away from fibres. The near-interface matrix morphology is largely affected by the pitch flow nature during mesophase transition, which is sensitive to the local preform geometry.

The fibre–matrix interface is generally microfissured. Numerous microcracks are observed both within matrix and along the partially bonded interface. The microcracks along the interface have an irregular shape which readily outline the fibre surface topography. The sharp, lenticular-shaped microcracks within matrix are formed between and parallel to the basal planes of the matrix platelets. These circumferential submicron-sized matrix cracks appear smaller and denser near the interface.

Acknowledgement

The authors would like to thank Ms. Karla Rankin for careful typing of this manuscript.

References

1. A. OBERLIN, in Proceedings of the Third Materials Technology Center's Conference on Solid Carbon Materials: Production and Properties, Carbondale, IL (Materials Technology Center, Carbondale, IL) p. 163.
2. D. CRAWFORD and D. J. JOHNSON, *J. Microscopy* **94** (1971) 51.
3. S. C. BENNETT and D. J. JOHNSON, *Carbon* **17** (1979) 25.
4. I. MOCHIDA, I. ITO, Y. KORAI, H. FUJITSU and K. TAKESHITA, *Carbon* **19** (1981) 457.
5. D. J. JOHNSON, D. CRAWFORD and B. F. JONES, *J. Mater. Sci.* **8** (1973) 286.
6. X. BOURRAT, E. J. ROCHE and J. G. LAVIN, *Carbon* **28** (1990) 236.
7. H. MARSH, *Fuel* **52** (1973) 205.
8. M. SHIRAISHI, G. TERRIERE and A. OBERLIN, *J. Mater. Sci.* **13** (1978) 702.
9. D. AUGUIE, M. OBERLIN, A. OBERLIN and P. HYVERNAT, *Carbon* **18** (1980) 337.
10. H. MARSH and D. CRAWFORD, *Carbon* **22** (1984) 413.
11. S. DeFONTON, A. OBERLIN and M. INAGAKI, *J. Mater. Sci.* **15** (1980) 909.
12. M. INAGAKI, A. OBERLIN and S. DEFONTON, *High Temp. High Pressures* **9** (1977) 453.
13. J. GOMA and A. OBERLIN, *Carbon* **23** (1985) 85.
14. J. N. ROUZAUD and A. OBERLIN, *Thin Solid Films* **105** (1983) 75.
15. M. HUTTEPAIN and A. OBERLIN, *Carbon* **28** (1990) 103.
16. P. EHRBURGER and J. LAHAYE, *Carbon* **19** (1981) 1.
17. J. DON and C. P. JU, *Mater. Sci. Engng* **A124** (1990) 259.
18. E. FITZER, W. HÜTTNER and L. M. MANOCHA, *Carbon* **18** (1980) 291.
19. S. M. OH and J. Y. LEE, *Carbon* **26** (1988) 769.
20. J. E. ZIMMER and J. L. WHITE, *Carbon* **21** (1983) 323.
21. J. H. CRANMER, I. G. PLATZKER, L. H. PEEBLES and D. R. UHLMAN, *Carbon* **21** (1983) 201.
22. R. A. MEYER and S. R. GYETVAY, in "Petroleum derived carbons", ACS Symposium Vol. 303, edited by J. D. Bacha, J. W. Newman, and J. L. White (American Chemical Society, Washington, D.C. 1986) p. 380.
23. N. MURDIE, J. DON, W. KOWBEL, P. SHPIK and M. A. WRIGHT, Personal Communications.
24. C. P. JU, Unpublished research.
25. L. H. PEEBLES Jr., R. A. MEYER and J. JORTNER, in Proceedings of Second International Conference on Composite Interfaces (ICCI-1), Cleveland, June 1988, edited by H. Ishida (Elsevier, New York) p. 1.
26. J. JORTNER, *Carbon* **24** (1986) 603.
27. M. A. FORREST and H. MARSH, *J. Mater. Sci.* **18** (1983) 973.
28. S. RAGAN and H. MARSH, *J. Mater. Sci.* **18** (1983) 3712.
29. K. Y. SOHN, SEH-MIN OH and JAI-YOUNG LEE, *Carbon* **26** (1988) 157.

Received 2 July 1990
and accepted 31 January 1991